Article

The Transcriptional Repressor PerR Senses Sulfane Sulfur by Cysteine Persulfidation at the Structural Zn²⁺ Site in *Synechococcus* sp. PCC7002

Daixi Liu [1,2,3]**, Hui Song** [1,3,]*****, Yuanning Li** [1,3]**, Ranran Huang** [1,3]**, Hongyue Liu** [1,3]**, Kunxian Tang** [4]**, Nianzhi Jiao** [1,3] **and Jihua Liu** [1,3]

[1] Institute of Marine Science and Technology, Shandong University, Qingdao 266237, China
[2] School of Pharmaceutical Sciences, Shandong University, Jinan 250012, China
[3] Joint Lab for Ocean Research and Education at Dalhousie University, Shandong University and Xiamen University, Qingdao 266237, China
[4] Third Institute of Oceanography, Ministry of Natural Resources, Xiamen 361000, China
***** Correspondence: 201799900009@sdu.edu.cn; Tel.: +86-137-089-966-21

Abstract: Cyanobacteria can perform both anoxygenic and oxygenic photosynthesis, a characteristic which ensured that these organisms were crucial in the evolution of the early Earth and the biosphere. Reactive oxygen species (ROS) produced in oxygenic photosynthesis and reactive sulfur species (RSS) produced in anoxygenic photosynthesis are closely related to intracellular redox equilibrium. ROS comprise superoxide anion ($O_2^{\bullet-}$), hydrogen peroxide (H_2O_2), and hydroxyl radicals ($^\bullet OH$). RSS comprise H_2S and sulfane sulfur (persulfide, polysulfide, and S_8). Although the sensing mechanism for ROS in cyanobacteria has been explored, that of RSS has not been elucidated. Here, we studied the function of the transcriptional repressor PerR in RSS sensing in *Synechococcus* sp. PCC7002 (PCC7002). PerR was previously reported to sense ROS; however, our results revealed that it also participated in RSS sensing. PerR repressed the expression of *prxI* and downregulated the tolerance of PCC7002 to polysulfide (H_2S_n). The reporter system indicated that PerR sensed H_2S_n. Cys^{121} of the $Cys4:Zn^{2+}$ site, which contains four cysteines (Cys^{121}, Cys^{124}, Cys^{160}, and Cys^{163}) bound to one zinc atom, could be modified by H_2S_n to Cys^{121}-SSH, as a result of which the zinc atom was released from the site. Moreover, Cys^{19} could also be modified by polysulfide to Cys^{19}-SSH. Thus, our results reveal that PerR, a representative of the Cys_4 zinc finger proteins, senses H_2S_n. Our findings provide a new perspective to explore the adaptation strategy of cyanobacteria in Proterozoic and contemporary sulfurization oceans.

Keywords: cyanobacteria; sulfane sulfur; PerR; peroxiredoxin; transcriptional regulator

1. Introduction

The environment on Earth transformed from anaerobic to aerobic during the evolution of life [1]. Cyanobacteria, some of the oldest microorganisms on Earth that can perform both anoxygenic and oxygenic photosynthesis, were a key driving force during evolution [2]. Life is created, regulated, and sustained by reduction–oxidation (redox) reactions, and ROS and RSS are two critical kinds of signal intracellular molecules associated with the redox balance [3]. In Proterozoic oceans, cyanobacteria perform anoxygenic photosynthesis, using alternative reduced electron donors, such as hydrogen sulfide (H_2S) [4]. Therefore, RSS should be the major participant in the regulation of the intracellular redox balance in cyanobacteria. Oxygenic photosynthesis, which uses solar energy to pry electrons from water, became a major part of the Earth's ecosystems as it succeeded in oxygenating the atmosphere and the biosphere more than 3 billon years (Ga) ago [5]. The main player in redox regulation became ROS. Although the modern ocean is aerobic, there are still some areas that lack oxygen, such as oxygen-minimum zones [6] and microbial mats [7].

The versatility of cyanobacteria to perform both anoxygenic photosynthesis and oxygenic photosynthesis has therefore been conserved [8], with cyanobacteria coping with both ROS and RSS in living environments. The metabolic regulation mechanism of ROS in cyanobacteria has widely been reported [9–11]; however, the sensing mechanisms of RSS have remained incompletely understood.

RSS, similar to ROS, are important cellular signaling molecules [3]. ROS comprise $O^{2\bullet-}$, H_2O_2, and hydroxyl radicals ($^\bullet OH$), which are products of molecular oxygen accepting electrons from cellular redox components [12]. H_2S and sulfane sulfur are representatives of RSS, which are produced during the process of sulfur-containing compound metabolism [13–15]. Even though H_2S was originally thought to be a gasotransmitter [16], emerging evidence suggests that sulfane sulfur plays a more important role in signal transduction [17–20]. Sulfane sulfur consists of various forms of zero-valent sulfur, including persulfide forms (RSSH and HSSH), polysulfide forms (RSS_nH, RSS_nR, and H_2S_n, $n \geq 2$), and elemental sulfur (S_8). Sulfane sulfur operates via a similar mechanism to ROS while acting as a signaling molecule, namely, by modifying protein at a cysteine residue. In addition, the second and equally important mechanism would be performed by reacting with metal centers in proteins [21]. S-sulfhydration could protect cysteine residues from ROS-mediated damaging oxidation [22]. However, excess sulfane sulfur can initiate complex antioxidant reactions, even affecting cellular processes, which is catastrophic for cellular function [23]. Furthermore, sulfane sulfur participates in the regulation of gene expression in photosynthesis [24]. Therefore, it is important to maintain intracellular sulfane sulfur homeostasis.

Microorganisms have evolved a series of protective enzymes to maintain intracellular sulfane sulfur concentration within safe limits. Sulfide:quinone oxidoreductase (SQR) [15], persulfide dioxygenase (PDO) [25], and flavocytochrome c sulfide dehydrogenase (FCSD) [26] are involved in the process. Under normal conditions, SQR oxidizes H_2S and produces sulfane sulfur, which is further oxidized by PDO. FCSD is another type of enzyme that also oxidizes H_2S. However, some ROS coping strategies were also reported to be suitable for sulfane sulfur, such as superoxide dismutases (SOD), catalase, thioredoxin (Trx), glutaredoxin (Grx), and peroxiredoxin (Prx). SOD was reported to metabolize H_2S and produce RSS, and catalase could also act as a H_2S oxidase [27–29]. Trx, Grx and Prx systems also participate in the process of sulfane sulfur reduction [30,31]. Thus, there is a close relationship between RSS and ROS metabolism.

The response to sulfane sulfur in bacteria is often coordinated by transcription factors [32]. CstR [33], BigR [34], SqrR [35], and FisR [36] are major transcription factors. CstR, BigR, and SqrR are transcription repressors, negatively regulating the transcription of H_2S oxidation-related genes, while FisR is a σ^{54}-dependent transcription activator. These regulatory factors display a similar mechanism of RSS sensing; that is, RSS modifies the two cysteines on the protein to form a Cys-S-S-Cys structure. OxyR was also reported to participate in sulfane sulfur sensing [30]. *Escherichia coli* OxyR was the earliest transcription factor discovered; it regulates the expression of *katG* (encoding catalase), *trxC* (encoding Trx), and *grxA* (encoding Grx). OxyR is a transcriptional activator that acts via the formation of a disulfide bond between the C^{199} and C^{208} residues, while sensing H_2O_2 [37]. Sulfane sulfur modifies OxyR at Cys^{199} and forms a persulfide OxyR Cys^{199}-SSH, thus activating the expression of the *trx* and *grx* genes. PerR is another type of peroxide-sensing regulator, which is complementary to OxyR; therefore, these two regulators do not usually exist in the same bacterium. PerR, which belongs to the Fur family, is a metal-dependent regulator that represses the expression of oxidative stress genes (*prx* and *ahpc*) [38,39]. PerR contains a DNA-binding region, a Zn^{2+}-binding site consisting of cysteine residues, and a Fe^{2+}/Mn^{2+}-binding site consisting of histidine and aspartic acid residues. Based on the above, we deduced that PerR may also be involved in sulfane sulfur sensing, but the mechanism may be different from that of OxyR. This hypothesis remains to be explored.

Many studies have focused on the role of PerR in H_2O_2 sensing, but the mechanism of sulfane sulfur sensing is still unclear. Li et al. found that PerR in *Synechocystis* sp. PCC6803

binds to the promoter region of *prx* to regulate its expression in response to peroxide stress [9]. Ludwig et al. found that *prx* expression in PCC7002 was also regulated by PerR [40]. However, these studies did not resolve the specific regulation mechanism of PerR. The mechanism by which PerR senses H_2O_2 in *Bacillus subtilis* has been reported in detail. *B. subtilis* PerR contains a structural metal ion (Zn^{2+}) binding site and a regulatory metal ion (Fe^{2+} or Mn^{2+}) binding site. In the presence of excess H_2O_2 or O_2, the two histidines that constitute the binding site of regulatory metal ions are oxidized, and the inhibitory effect of PerR is released. This is the main mechanism by which PerR senses H_2O_2 [38]. In addition, four conserved cysteines combine with Zn^{2+} to form a $Cys_4:Zn^{2+}$ structure, which also plays a key role in the process of redox regulation [39]. Based on this mechanism of H_2O_2 sensing and considering that the site of action of sulfane sulfur is cysteine [41], we speculated that the active site of sulfane sulfur on PerR may be the $Cys_4:Zn^{2+}$ structure. It has not been reported how, or indeed whether, the $Cys_4:Zn^{2+}$ structure is affected by sulfane sulfur, and thus, the mechanism needs to be explored in greater depth.

Here, we report that *Synechococcus* PerR senses sulfane sulfur and regulates the expression of *prxI*. PerR effectively decreases the tolerance of PCC7002 to sulfane sulfur by altering the expression of *prxI*. Sulfane sulfur modifies Cys^{19} and Cys^{121} to form Cys^{19}-SSH and Cys^{121}-SSH; as a result, the zinc atom is released from the $Cys_4:Zn^{2+}$ site, destroying the function of PerR. The discovery that sulfane sulfur acts on the $Cys_4:Zn^{2+}$ site of regulators is significant. Our findings reveal a new sulfane sulfur sensing mechanism, and provide a new perspective for exploring the adaptive mechanism of cyanobacteria in the evolution from an anaerobic environment to an aerobic one on Earth and the contemporary anoxic environment.

2. Materials and Methods

2.1. Strains and Culture Conditions

PCC7002 and its mutants (PCC7002Δ*perR* and PCC7002Δ*prxI*Δ*perR*) were grown in conical flasks containing medium A$^+$ [42] under continuous illumination of 50 μmol photons m^{-2}·s^{-1}, at 30 °C. To sustain normal growth, 30 μg/mL chloramphenicol was added to the medium of PCC7002Δ*perR*, and 50 μg/mL kanamycin and 30 μg/mL chloramphenicol were added to the medium of PCC7002Δ*prxI*Δ*perR*. *Escherichia coli* strains were cultured in LB medium, at 37 °C. All strains and plasmids are listed in Table S1.

2.2. Construction of PCC7002 Mutants

The PCC7002Δ*prxI* mutant was constructed in our previous study [31]. PCC7002Δ*perR* and PCC7002Δ*prxI*Δ*perR* were constructed by natural transformation and homologous recombination according to a previously reported method [24]. The plasmid used in *perR* deletion was constructed as follows. First, two segments, ~1000-bp long, immediately upstream and downstream of the *perR* gene, were acquired using the primer sets *perR*-del-1/*perR*-del-2 and *perR*-del-5/*perR*-del-6 (Table S2) by PCR from genomic DNA of PCC7002. The chloramphenicol resistance cartridge was amplified with the primers *perR*-del-3/*perR*-del-4. Second, the above three segments were fused by PCR, and they were connected with the pJET1.2 blunt vector by the TEDA method [43]. Then, the product was transformed into *E. coli* DH5α by electroporation, and correct transformants were verified by PCR and sequencing. For PCC7002Δ*perR*, the correct plasmid was transformed into PCC7002 by natural transformation. For PCC7002Δ*prxI*Δ*perR*, the correct plasmid was transformed into PCC7002Δ*prxI*. Here, 30 μg/mL chloramphenicol was used to select for correct transformants. Finally, the mutants PCC7002Δ*perR* and PCC7002Δ*prxI*Δ*perR* were verified by PCR and sequencing.

2.3. The Toxicity of H_2S_n against PCC7002, PCC7002Δ*perR*, and PCC7002Δ*prxI*Δ*perR*

H_2S_n, at concentrations of 1, 3, and 5 mM, was added to the sealed centrifugation tubes containing PCC7002, PCC7002Δ*perR*, and PCC7002Δ*prxI*Δ*perR* cells at log phase with

an OD_{730nm} of 0.6–0.7. H_2S_n was prepared according to a previously reported method with minor modification [15]. Briefly, sulfur powder, NaOH, and NaHS were mixed in a 1:1:1 molar ratio and dissolved in distilled water under argon gas in sealed bottle. Then, the bottle was incubated, at 37 °C, till sulfur was completely dissolved. After 6 h incubation, at 30 °C, under continuous illumination of 50 μmol photons·m^{-2}·s^{-1}, cells were washed and resuspended in fresh A^+ medium. Then, 10 μL of cells was placed on the A^+ agar plate after diluting with A^+ medium to 10^0, 10^{-1}, and 10^{-2}. The plates were cultivated at 30 °C under continuous illumination of 50 μmol photons·m^{-2}·s^{-1} for 7 days.

2.4. Induction, RNA Extraction, and qRT-PCR Analysis

PCC7002 and PCC7002Δ*perR* cells at log phase with an $OD_{730\,nm}$ of 0.6–0.7 were incubated with or without H_2S and H_2S_n (at concentrations of 250 and 500 μM) in sealed centrifuge tubes for 3 h, at 30 °C, and 50 μmol photons·m^{-2}·s^{-1} illumination. H_2S was prepared according to the previous report [44] and experimental requirements, and the preparation method was as follows: 56.06 mg NaHS was dissolved into 1 mL of buffer (containing 50 mMTris.HCL and 100 μM DTPA), which had been degassed with N_2 prior to NaHS powder solubilization, and diluted according to the desired concentration. Then, the induced cells were harvested by centrifugation at $10,000 \times g$, and 4 °C for 10 min. Total RNA was isolated using the TaKaRa MiniBEST Universal RNA Extraction Kit, and the concentration and quality of RNA were verified by Qubit 4 (Invitrogen, Carlsbad, CA, USA). The cDNA was acquired using the Prime Script™ RT reagent kit with gDNA Eraser (TaKaRa, Dalian, China). qRT-PCR was performed using the CFX96 Touch Real-Time PCR Detection System (Bio-Rad, Hercules, CA, USA) with the SYBR® Premix Ex Taq™ II kit (TaKaRa, Dalian, China). The primers used for the target genes are shown in Table S1. The reference gene *rnpA* (SYNPCC7002_A0989) was also included [45]. The results were analyzed according to the $2^{-\Delta\Delta CT}$ method [46].

2.5. Construction of the perR-Repressed Reporter System

A perR-repressed reporter system in *E. coli* BL21 was constructed to assess the regulatory role of PerR on *prxI* expression. The plasmid pBBR-*perR*-P*prxI*-*egfp* was constructed as follows: The *perR* gene was expressed under the control of the *lacI* promoter, and the *egfp* gene was expressed under the control of the *prxI* promoter. PerR could act on the promoter region of *prxI*, thus influencing the fluorescence of GFP. The effect of H_2S_n and S_8 on PerR were evaluated by the changes in fluorescence intensities. The plasmid was transformed to *E. coli* BL21 for further study. *E. coli* BL21 (pBBR-*perR*-P*prxI*-*egfp*) was cultured in LB media, at 37 °C, to logarithmic phase ($OD_{600nm} = 0.6$) and 0.5 mM of isopropyl β-D-thiogalactoside (IPTG) was added to induce *PerR* expression. Then, H_2S, H_2S_n, and S_8 (at concentrations of 0, 150, and 300 μM) were added to the medium and the cells were cultured for another 2 h. Finally, the cells were collected and washed twice with 50 mM PBS (pH 7.4) to detect the fluorescence of GFP at excitation and emission wavelengths of 482 nm and 515 nm.

The six cysteines of PerR in the pBBR-*perR*-P*prxI*-*egfp* plasmid were all mutated to serines using the primer pairs PerR-C19S-F/R, PerR-C121S-F/R, PerR-C124S-F/R, PerR-C137S-F/R, PerR-C160S-F/R, and PerR-C163S-F/R by a modified QuickChange Site-Directed Mutagenesis Method [47]. *E. coli* BL21 (pBBR-*perR*$_{C-S}$-P*prxI*-*egfp*) cells at logarithmic phase were induced with 0.5 mM IPTG and incubated with 300 μM H_2S_n for 2 h to investigate the role of cysteines in PerR.

2.6. Construction, Overexpression, and Purification of PerR

PerR was fused to the C-terminus of maltose binding protein (MBP) and overexpressed in the vector pMal-C2X [48]. To achieve this, the perR fragment was amplified from the PCC7002 genome using the primer pair pMal-*perR*-F/R, ligated to pMal-C2X by the TEDA method, and transformed into *E. coli* DH5α. Verified plasmid was then transformed into *E. coli* BL21(DE3), and the resulting pMal-*perR* cells were cultured in LB medium, at 37 °C, to an OD_{600nm} of 0.6. Then, 0.5 mM IPTG was added for an additional 6 h incubation, at 30 °C.

The cells were disrupted by a pressure cell homogenizer (SPCH-18; Stansted Fluid Power Ltd., London, UK). The cell debris was removed by centrifugation at $13,000\times g$ and 4 °C for 20 min. PerR protein with the MBP (MBP-PerR) was separated by Amylose Resin Column (Invitrogen, Carlsbad, CA, USA) according to the supplier's recommendations. PerR was released from the fusion with MBP using Factor Xa, at room temperature, for 24 h.

2.7. Zn^{2+} Release Assay

PAR could bind to Zn^{2+} and the Zn^{2+}-PAR complex had maximum absorption at 494 nm; thus, absorption was used to indicate the amount of Zn^{2+}. Here, 5 µM of purified PerR was treated with 10 mM H_2S_n or 10 mM H_2O_2 in the presence of 100 µM PAR at 25 °C, and released Zn^{2+} ions were measured by monitoring the Zn^{2+}-PAR complex at 494 nm every 1 s for 10 min. PerR without treatment was used as a control.

2.8. LC-MS/MS Analysis of PerR

Purified PerR at 5 mg/mL was reacted with 1 mM H_2S_n sulfur or DTT for 30 min, at 25 °C. The reacted protein was treated with denaturing buffer (0.5 M Tris-HCl, 2.75 mM EDTA, 6 M guanadine-HCl, pH 8.0), then incubated with 1 M iodoacetamide (IAM) for 1 h in the dark. The sample was subsequently digested with trypsin (1:25, w/w), at 37 °C, for 20 h and subjected to C18 Zip-Tip (Millipore, Burlington, MA, USA) purification for desalting before analysis by HPLC-tandem mass spectrometry (LC-MS). A gradient of solvent A (0.1% formic acid in 2% acetonitrile) and solvent B (0.1% formic acid in 98% acetonitrile) from 0% to 100% in 100 min was used for elution in the Prominence nano-LC system (Shimadzu, Kyoto, Japan). LTQ-OrbitrapVelos Pro CID mass spectrometer (Thermo Scientific, Waltham, MA, USA) was used to ionize and electrospray the eluent, which was run in data-dependent acquisition mode with Xcalibur 2.2.0 software (Thermo Scientific, Waltham, MA, USA). Fullscan MS spectra (from 400 to 1800 m/z) were detected in the Orbitrap with a resolution of 60,000 at 400 m/z [17,36,49–52].

2.9. Phylogenetic Analysis

Cyanobacterial genomes were downloaded from the NCBI database. The sequences in Table S3 were used as queries to obtain PerR candidates. The candidates were obtained by searching the database with the standalone BLASTP algorithm, using conventional criteria (E value of $\geq 1 \times 10^{-5}$ coverage of $\geq 45\%$, and identity of $\geq 30\%$) [53]. PerR candidates were aligned using MAFFT version 7.490 [54] with the option "-auto-maxiterate 1000", and ambiguously aligned regions were removed using trimAl version 1.4 [55] with the "gappyout" option. Phylogenetic analysis was performed based on maximum likelihood methods using IQ-TREE [56] with automatic detection of the best-fit model with the "-MFP" option using ModelFinder [57] under the Bayesian information criterion (BIC). The topological robustness of the tree was evaluated by 1000 ultrafast bootstrap replicates. PerR proteins from *Staphylococcus epidermidis*, *Staphylococcus haemolyticus*, and *Staphylococcus aureus*, detailed in Table S3 were used as an outgroup.

3. Results

3.1. Phylogenetic Analysis of PerR in Cyanobacteria

To investigate the distribution of PerR in cyanobacteria, we performed a BLASTsearch of the 198 cyanobacteria genomes (downloaded from the NCBI database on 17 December 2021) with the queries (Table S3) to find PerR candidates (Figure 1). *PerR* genes were identified using phylogenetic tree analysis (Figure 1A). In total, 68 PerR-encoding genes were distributed among 64 cyanobacteria genomes (Table S4). The cyanobacteria PerRs were distributed among five orders, including 25 *Synechococcales*, 27 *Nostocales*, 3 *Gloeobacteria*, 9 *Oscillatoriales*, and 4 *Pseudanabaenales* (Figure 1B). In *Gloeobacteria*, which was believed to be the early diverging lineage of cyanobacteria, all three of the published genomes within this order were encoded as *perR*. Furthermore, the proportions of species that contained *perR* in *Oscillatoriales* and *Nostocales* were 81.8% and 56.3%, respectively. For

Synechococcales, the proportion was 27.5%, even though the total number of *PerR* genes was 25. For *Pseudanabaenales*, the proportion was only 23.5%.
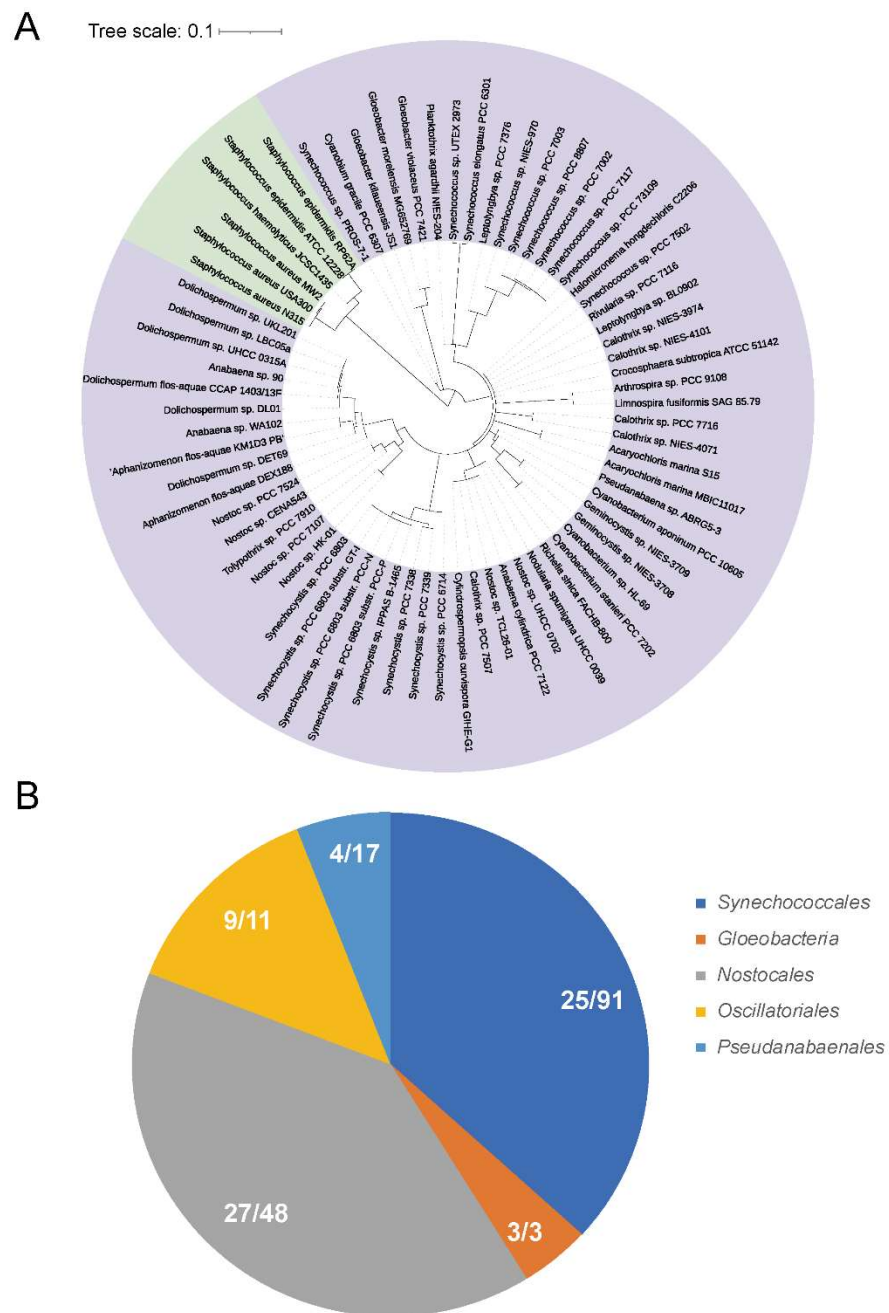

Figure 1. Phylogenetic analysis of PerR-encoding genes in the sequenced cyanobacteria genomes. (**A**) Phylogenetic tree of PerRs in cyanobacteria. A total of 68 probable PerRs were found in 198 cyanobacteria genomes. The representative proteins were labeled with name of species. The PerR queries were listed in Table S3. PerRs from *Staphylococcus epidermidis*, *Staphylococcus haemolyticus* and *Staphylococcus aureus* in Table S3 were used as the outgroup. (**B**) The distribution of PerR-encoding genes in cyanobacteria genomes. In total, 68 predicted PerR-encoding genes were detected among 64 cyanobacteria genomes, including 25 *Synechococcales*, 27 *Nostocales*, 3 *Gloeobacteria*, 9 *Oscillatoriales*, and 4 *Pseudanabaenalles*.

3.2. PerR Deletion Increases the Tolerance of PCC7002 to High H_2S_n

To investigate the effect of PerR on the tolerance of PCC7002 to sulfane sulfur, we constructed a single-deletion strain PCC7002$\Delta perR$, and double-deletion strain PCC7002$\Delta prxI$

$\Delta perR$ by homologous recombination (Figure S1). The mutation was verified by PCR (Figure S1A). Then, the tolerance of PCC7002, PCC7002$\Delta perR$, and PCC7002$\Delta prxI\Delta perR$ to sulfane sulfur was tested (Figure 2). PCC7002$\Delta perR$ grew better than the wild-type after induction with 5 mM H_2S_n, indicating that the deletion of *perR* increased tolerance (Figure 2A,B). However, the double-deletion mutant (PCC7002$\Delta prxI\Delta perR$) showed decreased tolerance to H_2S_n, and growth inhibition was apparent after induction with 3 mM H_2S_n (Figure 2C). These results indicated that PerR and PrxI were all involved in H_2S_n tolerance of PCC7002.
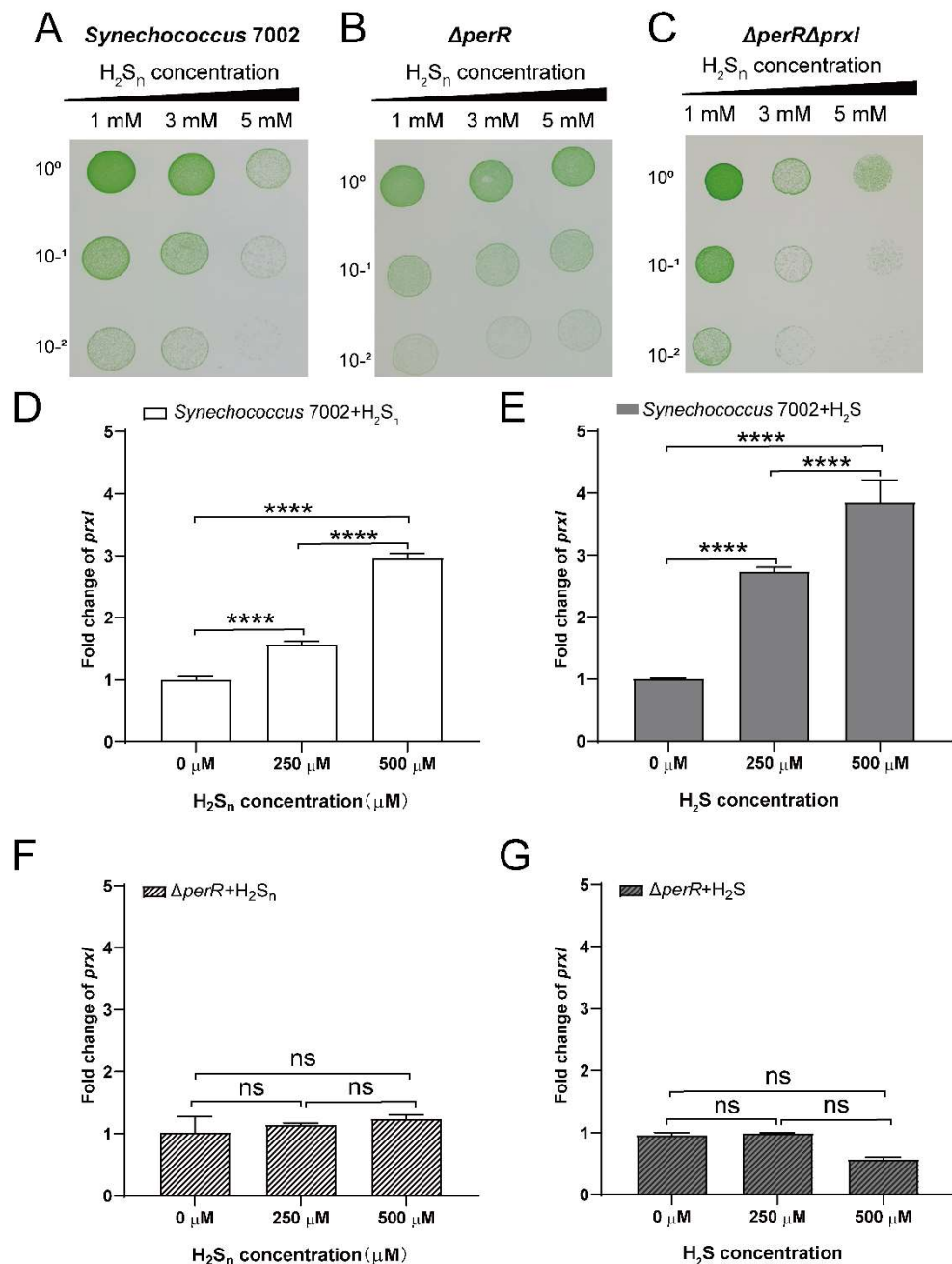

Figure 2. PerR decreases the tolerance of PCC7002 to H_2S_n. The deletion of *perR* (PCC7002$\Delta perR$) (**B**) increased H_2S_n tolerance, while the double deletion of *perR* and *prxI* (PCC7002$\Delta prxI\Delta perR$) (**C**) decreased H_2S_n tolerance compared with the wild–type (**A**). PCC7002, PCC7002$\Delta perR$, and PCC7002$\Delta prxI\Delta perR$ cells at log phase with an $OD_{730\ nm}$ of 1 were treated with 1, 3, and 5 mM H_2S_n, at 30 °C, and 50 µmol photons m^{-2}·s^{-1} illumination for 6 h. Then, cells were diluted with A$^+$ medium to 10^0, 10^{-1}, and 10^{-2}, and plated onto the A$^+$ solid medium and cultured for 7 days, at 30 °C, and 50 µmol photons·m^{-2}·s^{-1} illumination. The tolerance of PCC7002$\Delta perR$ and PCC7002$\Delta prxI\Delta perR$ to

H_2S_n was opposite to that of the wild-type. The expression of *prxI* was largely upregulated by H_2S_n (**D**) and H_2S (**E**) in PCC7002, while H_2S_n (**F**) and H_2S (**G**) showed little influence on its expression in PCC7002Δ*perR*. PCC7002 and PCC7002Δ*perR* cells at log phase were induced by H_2S_n and H_2S with concentrations of 250 μM and 500 μM for 3 h, and the expression of *prxI* was measured. The *Y*-axis is the fold change in *prxI* calculated by relative quantitative qPCR, based on the $2^{-\Delta\Delta CT}$ method, with *rnp* as the reference gene. All data are averages from three samples with standard deviations (error bars). The experiment was repeated at least three times. ****, $p < 0.0001$; ns, not significant (paired *t* test).

3.3. PerR Senses H_2S_n and Regulates the Expression of prxI

PerR acts as a transcriptional repressor in the regulation of *prxI* expression, as qPCR analysis showed that the transcript level of *prxI* was upregulated ~100-fold in PCC7002Δ*perR* compared with PCC7002 (Figure S1B). Furthermore, the expression levels of *prxI* were analyzed in PCC7002 and PCC7002Δ*perR* after induction with H_2S_n and H_2S to verify whether PerR is involved in the regulation of H_2S_n metabolism. The expression of *prxI* increased 1.5-fold following 250 μM H_2S_n induction and 3-fold following 500 μM H_2S_n induction (Figure 2D); this effect was concentration dependent. H_2S induction could also increase *prxI* expression by 2.5-fold at concentrations of 250 μM and 4-fold at concentrations of 500 μM (Figure 2E). However, neither H_2S nor H_2S_n could induce the expression of *prxI* in PCC7002Δ*perR* (Figure 2F,G), which was different from the wild-type. Based on the above results, we deduced that PerR played a critical role in H_2S_n sensing, thus regulating the expression of *prxI*.

Meanwhile, a PerR-repressed reporter system in *E. coli* BL21 was constructed to further assess the effect of H_2S_n on *prxI* expression regulated by PerR (Figure 3). In the reporter system, the *perR* gene is controlled by the *lacI* promoter (PlacI), and the *egfp* gene is controlled by the *prxI* promoter (P_{prxI}) (Figure 3A). When the expression of PerR was induced by IPTG, GFP fluorescence decreased significantly, indicating that the expressed PerR could act on the *prxI* promoter and inhibit the expression of GFP (Figure S2). Having verified that PerR acts on the promoter of *prxI* to inhibit its expression, the effects of H_2S_n and S_8 were tested. H_2S_n induction caused an increase in fluorescence intensity (Figure 2A), and S_8, another form of sulfane sulfur, had a similar effect (Figure 2B).

To test the critical role of Cys residues in PerR, all six Cys residues (Cys^{19}, Cys^{121}, Cys^{123}, Cys^{137}, Cys^{160}, and Cys^{163}) were individually mutated to Ser. The mutation of Cys^{19} and Cys^{137} (C19S and C137S) resulted in decreased fluorescence intensity but did not affect their response to H_2S_n. Cys^{121}, Cys^{124}, Cys^{160}, and Cys^{163} were important components of the $Cys_4:Zn^{2+}$ site, and their mutation to Ser (C121S, C124S, C160S, and C163S) resulted in increased fluorescence intensities compared with the wild-type, indicating the inactivation of PerR (Figure 3C). As a result, PerR no longer acted on the *prxI* promoter to inhibit the expression of *egfp*, and it no longer responded to H_2S_n induction. The mutation of His had no effect on PerR (Figure 3D), indicating H_2S_n did not act on the Fe^{2+}/Mn^{2+} site. We concluded that the expression of *prxI* was regulated by PerR, and the induction of S_8 and H_2S_n enhanced *prxI* expression by acting on PerR. Meanwhile, the Cys^{121}, Cys^{124}, Cys^{160}, and Cys^{163} residues of PerR played crucial roles in H_2S_n sensing.
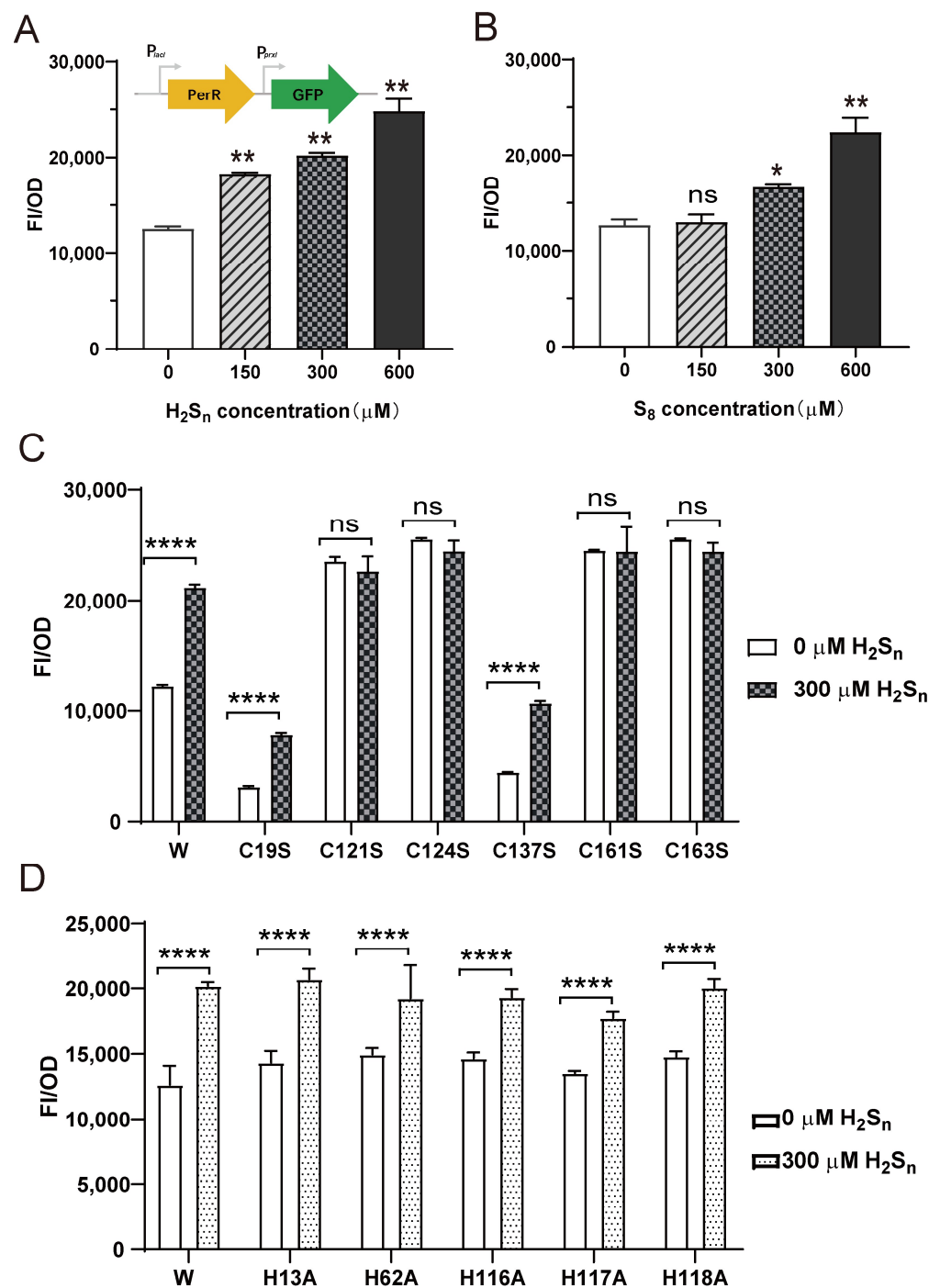
Figure 3. The effect of H_2S_n and S_8 on the PerR-repressed reporter. (**A**) Schematic representation of the test plasmid (pBBR-*perR*-P*prxI*-*egfp*). The expression of *egfp* was initiated by the *prxI* promoter (P*prxI*), and the interaction between PerR and P$_{prxI}$, which was associated with the inducers that affected GFP fluorescence. H_2S_n (**A**) and S_8 (**B**) induction increased the intensity of GFP fluorescence in *E. coli* BL21 (pBBR-*perR*-P*prxI*-*egfp*). (**C**) The mutation of Cys affected the function of PerR in *E. coli* BL21 (pBBR-*perR*-P*prxI*-*egfp*). C19S, C121S, C124S, C137S, C161S, and C163S represented single mutations of Cys to Ser in PerR. (**D**) The mutation of His did not affect the function of PerR in *E. coli* BL21 (pBBR-*perR*-P*prxI*-*egfp*). H13A, H62A, H116A, H117A and H118A represented single mutations of His to Ala in PerR. FI/OD represents the fluorescence intensity of per OD cells. All data are averages from three samples with standard deviations (error bars). The experiment was repeated at least three times. *, $p < 0.1$; **, $p < 0.01$; ****, $p < 0.0001$; ns, not significant (paired *t* test).

3.4. Sulfane Sulfur Acts on the $Cys_4:Zn^{2+}$ Site of PerR

　　Furthermore, we measured the rate at which Zn^{2+} ions were released from PerR:Zn in the presence of H_2S_n (Figure 4). An amount of 1 μM PerR contains about 0.125 μM Zn, 0.033 μM Fe and 0.006 μM Mn, as detected by ICP-MS. As the previous result (Figure 3D) confirmed that H_2S_n did not act on the Fe^{2+}/Mn^{2+} site, the effect on $Cys_4:Zn^{2+}$ site was monitored here. The formation of the colored Zn^{2+}-PAR complex, whose absorption maximum was observed at 494 nm, was used to monitor the release of Zn^{2+}. Thus, the Zn^{2+} release result showed that all selected concentrations of H_2S_n induced the release of Zn^{2+}. Based on the above results, we deduced the mechanism by which H_2S_n acts on PerR, which involves H_2S_n acting on the $Cys_4:Zn^{2+}$ site to dissociate Zn^{2+} from the active site, thus destroying the normal function of PerR.
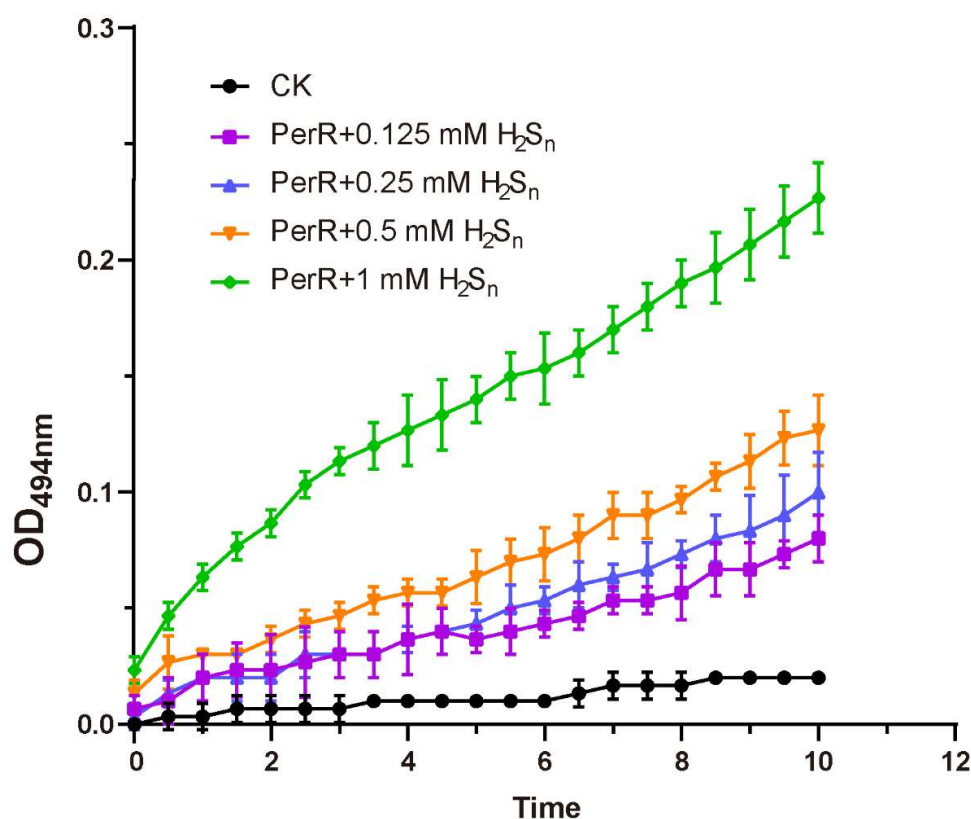

Figure 4. H_2S_n caused dissociation of zinc ions from PerR. Oxidation of the $Cys_4:Zn^{2+}$ site by H_2S_n led to Zn^{2+} release. H_2S_n was incubated with 100 μM PerR, and formation of the Zn^{2+}-PAR complex was continuously monitored by measuring the absorbance at 494 nm for 10 min. All data are averages from three samples with standard deviations (error bars). The experiment was repeated at least three times.

　　Finally, we explored the mechanism by which H_2S_n acts on the $Cys_4:Zn^{2+}$ site by LTQ-Orbitrap tandem mass spectrometry (Figure 5). Cys^{19}-SH of Peptide 1 in H_2S_n-treated PerR was modified to Cys^{19}-SSH (Figure 5A), while Cys^{19}-SH of Peptide 2 in DTT-treated PerR was directly modified by acetamide (CAM) (Figure 5B). Similarly, Cys^{121}-SH of Peptide 3 in H_2S_n-treated PerR was modified to Cys^{121}-SSH (Figure 5C), while Cys^{121}-SH of Peptide 4 in DTT-treated PerR was also directly modified by acetamide (CAM) (Figure 5D). Among these, Cys^{121} was an important constituent of the $Cys_4:Zn^{2+}$ site, thus indicating that H_2S_n acts on Cys^{121} to inhibit the activity of PerR. Notably, Cys^{19} was also modified by H_2S_n, although it was not a component of the $Cys_4:Zn^{2+}$ site. In summary, the persulfide modification of Cys^{121} in the $Cys_4:Zn^{2+}$ site by H_2S_n was the mechanism that affected PerR activity.
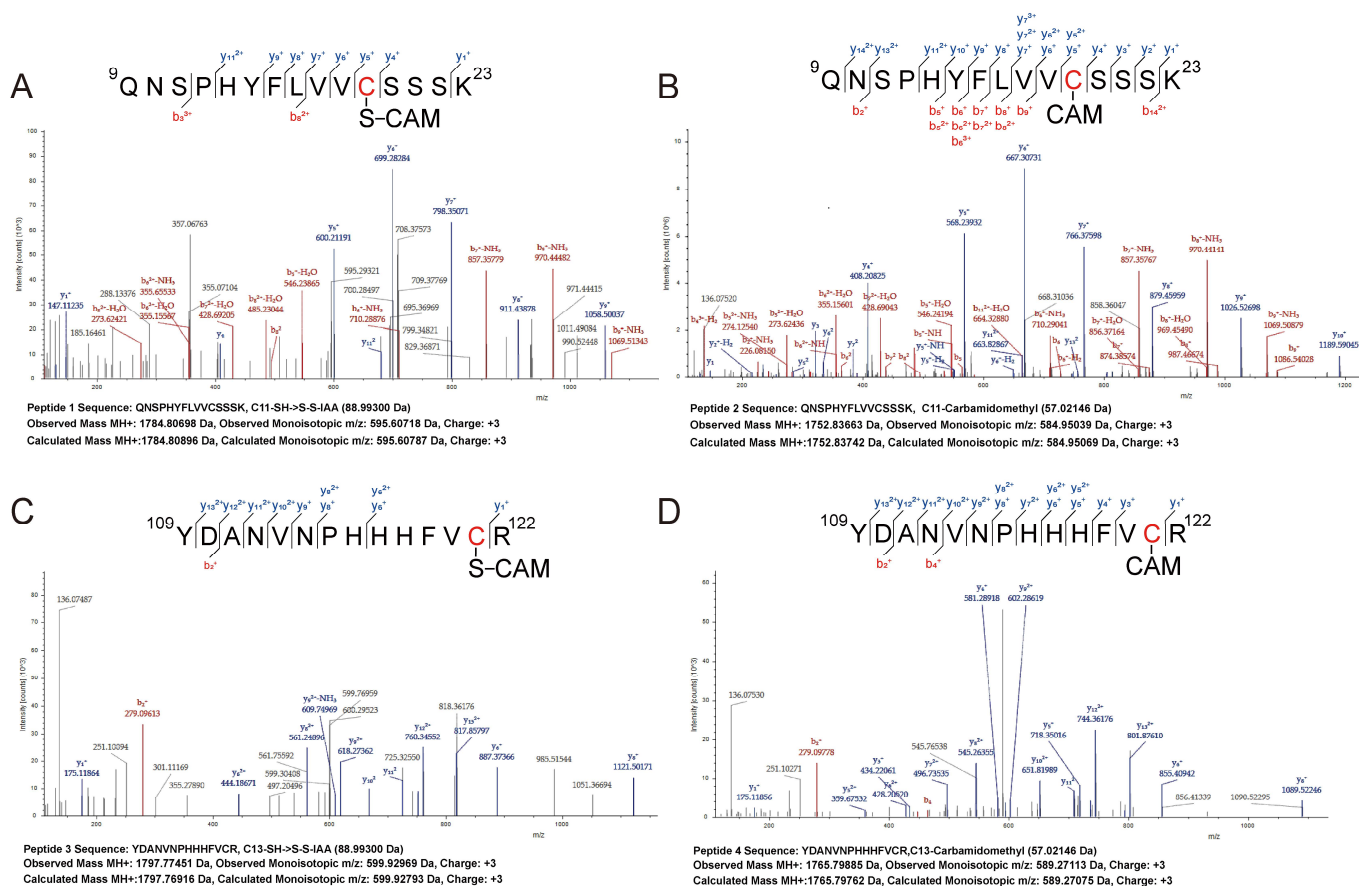
Figure 5. H_2S_n acted on the cysteines of PerR. (**A**) The Cys^{19}–SSH group was blocked by IAM in the peptide 1 from H_2S_n–treated PerR. (**B**) The Cys^{19}–SH group was blocked by IAM in the peptide 2 from DTT-treated PerR. (**C**) The Cys^{121}–SSH group was blocked by IAM in the peptide 3 from H_2S_n-treated PerR. (**D**) The Cys^{121}–SH group was blocked by IAM in the peptide 4 from DTT–treated PerR. The purified PerR (5 mg/mL) was treated with 1 mM H_2S_n and 1 mM DTT for 30 min, at 25 °C. After denaturing and incubating with IAM, the reacted protein was digested by trypsin. The generated peptides were detected by LTQ-Orbitrap tandem mass spectrometry.

4. Discussion

The data from our study revealed that PerR senses H_2S_n and regulates the expression of *prxI* (Figure 6). The deletion of *perR* increased the tolerance for H_2S_n in PCC7002 (Figure 2B), although the enhanced tolerance was not observed in the dual mutant PCC7002Δ*perR*Δ*prxI* (Figure 2C), indicating that PerR functioned by acting on PrxI. Meanwhile, the induction effect of H_2S_n on *prxI* transcription levels was only observed in the presence of PerR (Figure 2), a result which was further confirmed by the PerR-repressed reporter system (Figure 3), indicating that PerR acted on the promoter region to inhibit *prxI* expression. H_2S had similar effect with H_2S_n on *prxI* transcription levels (Figure 2B). This effect may be caused by H_2S_n, which derive from H_2S solution prepared from NaHS, as considerable levels of H_2S_n may present [44]. Meanwhile, H_2S may be converted to H_2S_n by SQR [24]. Certainly, H_2S may also act on PerR with a new mechanism directly, which needs to be further verified. Furthermore, H_2S_n acted on the Cys^4:Zn^{2+} site to release Zn^{2+}, thus removing the inhibition (Figure 4) and allowing *prxI* to be expressed in large quantities to clear the excess sulfane sulfur. H_2S_n modified Cys^{121} to form Cys^{121}–SSH (Figure 5), destroying the structure of the Cys^4:Zn^{2+} site and causing the release of Zn^{2+}. Cys^{19} could also be modified by H_2S_n. Thus, H_2S_n acted on the zinc figure structure of PerR, which represents a new type of mechanism for sulfane sulfur sensing.
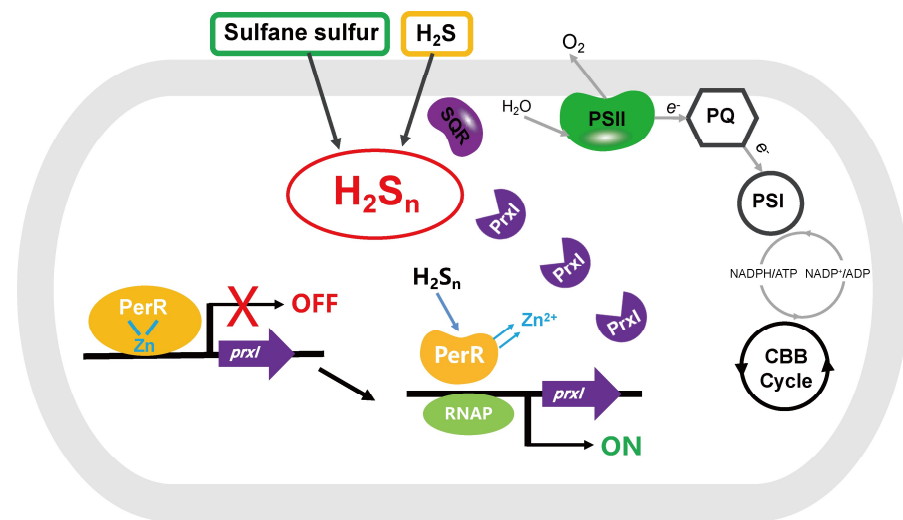
Figure 6. PerR senses H_2S_n and regulates the expression of *prxI* in PCC7002. H_2S_n induces the expression of *prxI* via PerR. PerR binds to Zn^{2+} and acts on the promoter of *prxI* to inhibit its expression, a process that can be disinhibited by H_2S_n. H_2S_n acts on the $Cys4:Zn^{2+}$ site of PerR to relieve Zn^{2+}, destroying the zinc finger structure. C^{121}-SH in the $Cys4:Zn^{2+}$ site is modified by H_2S_n and forms C^{121}-SSH.

Zinc-binding proteins are among the most abundant transcriptional regulators in eukaryotes, harboring at least one common motif, the zinc finger, which contributes to proper protein structure and function [58,59]. Zinc finger proteins are also found in prokaryotic genomes, such as *Bacillus* PerR [39] and *Synechococcus* PerR [9]. Zinc-binding proteins display variable secondary structures and vast functional diversity, and can be classified into three classes based on their distinct structural properties: Cys_2His_2 (C2H2) zinc finger proteins (Class I), Cys_4 (C4) zinc finger proteins (Class II), and Cys_6 (C6) zinc finger proteins (Class III). Class I proteins are often referred to as the classical zinc finger [60]. Class II proteins contain four cysteine residues bound to one zinc atom [61], whereas Class III proteins contain six cysteine residues bound to two zinc atoms [62]. Thus, *Synechococcus* PerR belongs to Class II, and this is the first report of a zinc-binding protein being involved in sulfane sulfur sensing.

OxyR and PerR are two representative regulators that can sense both H_2O_2 and H_2S_n. In total, 68 PerR proteins were identified among 198 sequenced cyanobacteria genomes (Figure 5), whereas only 9 OxyR proteins were identified (Table S5) [30], indicating that PerR may be the key player in cyanobacteria. Furthermore, PerR is a transcriptional inhibitor, whereas OxyR is a transcriptional activator, and their sensing mechanisms for H_2O_2 and H_2S_n are quite different. The exact mechanism for the OxyR sensing of H_2O_2 is still under debate. The formation of a disulfide bond between Cys^{199} and Cys^{208} or the oxidization of Cys^{199} to C^{199}-SOH in *E. coli* are two of the proposed mechanisms [63–65]. For H_2S_n sensing, the Cys^{199} of *E. coli* OxyR is modified to Cys^{199}-SSH [30]. *Bacillus* PerR senses H_2O_2 by metal-catalyzed oxidation [38], where one oxygen atom is incorporated into histidine 37 or histidine 91, which coordinates the bound Fe^{2+}. Cysteines in the $Cys_4:Zn^{2+}$ site may also be oxidized by H_2O_2 [39]. Our results revealed that Cys^{121} in the $Cys_4:Zn^{2+}$ site of *Synechococcus* PerR could be modified by H_2S_n to form Cys^{121}-SSH (Figure 4), releasing one zinc atom and destabilizing the structure. Normally, PerR and OxyR do not exist in the same microbial strain, but there are some exceptions [66,67]. In cyanobacteria, PerR and OxyR did not coexist (Tables S4 and S5). Thus, although PerR and OxyR are considered functionally complementary, the mechanisms by which they function are different.

In addition to OxyR and PerR, two-component systems play an important role in H_2O_2 signal transduction in cyanobacteria [68]. A microarray-based study in *Synechocystis* PCC6803 revealed that His kinases (Hiks), namely, Hik33, Hik34, Hik16, and Hik42, are involved in the expression of a large number of H_2O_2-inducible genes [10]. Among the four

Hiks, Hik33 was the main contributor and was responsible for the regulation of more H_2O_2-inducible genes than PerR. Furthermore, the response of *Synechocystis* to H_2O_2 treatment also relied on Group 2 sigma factors, namely, SigB and SigD [69]. The lack of Group 2 sigma factors meant that the strain was unable to sustain its growth under oxidative stress. Taken together, the signaling of H_2O_2-induced oxidative stress is based on the coordinated action of several regulators and dedicated alternative sigma factors. Whether these regulators participate in sulfane sulfur sensing requires further investigation.

The distribution of PerR proteins in cyanobacteria was also investigated. *Gloeobacterales* are early-branching photosynthetic cyanobacteria that are used as model species to study the physiology of early oxygenic phototrophs [70]. *Gloeobacterales* contain reduced photosystems that lack thylakoids and a circadian clock. However, our results revealed that all three species with published genomes within this order encoded *perR*, which may offer insight into the important role of PerR in primitive cyanobacteria and the evolution of oxygenic photosynthesis. Meanwhile, 81.8% of the species in *Oscillatoriales* and 56.3% of those in *Nostocales* contained PerR. *Oscillatoriales* and *Nostocales* are bloom-forming cyanobacteria that dominate among the cyanobacterial biomass of shallow polymictic eutrophic lakes [71]. The high proportion of PerR proteins among the two orders may provide insight into the survival strategies of cyanobacteria in hypoxic and sulfidic environments.

The finding that PerR senses H_2S_n in cyanobacteria is significant. First, cyanobacteria have to tolerate the accumulation of sulfane sulfur in living environments. In Proterozoic oceans [2] and modern oxygen minimum zones [72], the environments in which cyanobacteria thrive are anoxic and sulfidic, and as a result, sulfane sulfur might accumulate. In cyanobacteria mats, a typical habitat for these microorganisms, the cyanobacteria are intermittently exposed to sulfane sulfur [73]. Although cyanobacteria can perform sulfur respiration and provide ATP for growth under dark and anoxic conditions by reducing sulfane sulfur [74], excess sulfane sulfur is fatal to cells [23]. Therefore, PerR sensing of H_2S_n provides the opportunity for cyanobacteria to activate the expression of metabolic genes in time to scavenge excess sulfane sulfur, thus ensuring survival in such environments. Second, cyanobacteria perform anoxygenic photosynthesis under low-O_2 and sulfidic conditions, using H_2S as the electron donor [8,75]. In addition, cyanobacteria could produce some sulfur-containing histidine such as ergothioneine and ovothiols, which can also be used as electron donors [76,77]. As a result, sulfane sulfur was generated during the process of H_2S oxidation by SQR during anoxygenic photosynthesis. Sulfane sulfur is a signal that participates in the regulation of physiology and critical gene expression in photosynthesis [24]. The PerR sensing of H_2S_n may help cyanobacteria to maintain normal signal transduction and photosynthesis. Third, a previous study reported that the composition and stability of the photosynthetic machinery and the cell division process were affected by the overexpression of PerR [78], indicating that the effect of sulfane sulfur on the function of PerR may also affect the above process. Thus, the association between PerR, sulfane sulfur, photosynthesis, and cell division provides a new perspective on the significance of the PerR sensing of sulfane sulfur. In brief, the ability of PerR to sense H_2S_n may ensure that cyanobacteria respond to intracellular and extracellular sulfane sulfur in a timely manner, allowing them to maintain normal photosynthesis and cell division, and adapt to environmental conditions.

5. Conclusions

In summary, we showed that PerR in PCC7002 senses H_2S_n and regulates the expression of *prxI*. PCC7002 was able to respond in a timely manner to excess H_2S_n in the environment with the help of PerR, enhancing its tolerance. H_2S_n modified Cys^{121} of PerR to form Cys^{121}-SSH, thus releasing Zn^{2+} from the Cys_4:Zn^{2+} site, revealing a new mechanism of sulfane sulfur sensing in cyanobacteria. This is also the first report of a zinc-binding protein that participates in sulfane sulfur sensing. Our findings offer new insight into the mechanism of sulfane sulfur sensing and provide a new perspective for understanding the adaptation mechanism of cyanobacteria in anaerobic and sulfidic environments.

References

1. Schopf, J.W. Geological evidence of oxygenic photosynthesis and the biotic response to the 2400–2200 ma "great oxidation event". *Biochem. Biokhimiia* **2014**, *79*, 165–177. [CrossRef]
2. Soo, R.M.; Hemp, J.; Parks, D.H.; Fischer, W.W.; Hugenholtz, P. On the origins of oxygenic photosynthesis and aerobic respiration in Cyanobacteria. *Science* **2017**, *355*, 1436–1440. [CrossRef]
3. Olson, K.R. Reactive oxygen species or reactive sulfur species: Why we should consider the latter. *J. Exp. Biol.* **2020**, *223*, 196352. [CrossRef]
4. Johnston, D.T.; Wolfe-Simon, F.; Pearson, A.; Knoll, A.H. Anoxygenic photosynthesis modulated Proterozoic oxygen and sustained Earth's middle age. *Proc. Natl. Acad. Sci. USA* **2009**, *106*, 16925–16929. [CrossRef]
5. Buick, R. When did oxygenic photosynthesis evolve? *Philos. Trans. R. Soc. Lond. Ser. B Biol. Sci.* **2008**, *363*, 2731–2743. [CrossRef]
6. Oschlies, A. A committed fourfold increase in ocean oxygen loss. *Nat. Commun.* **2021**, *12*, 2307. [CrossRef]
7. Haas, S.; de Beer, D.; Klatt, J.M.; Fink, A.; Rench, R.M.; Hamilton, T.L.; Meyer, V.; Kakuk, B.; Macalady, J.L. Low-light anoxygenic photosynthesis and Fe-S-Biogeochemistry in a microbial mat. *Front. Microbiol.* **2018**, *9*, 858. [CrossRef]
8. Klatt, J.M.; Al-Najjar, M.A.; Yilmaz, P.; Lavik, G.; de Beer, D.; Polerecky, L. Anoxygenic photosynthesis controls oxygenic photosynthesis in a cyanobacterium from a sulfidic spring. *Appl. Environ. Microbiol.* **2015**, *81*, 2025–2031. [CrossRef]
9. Li, H.; Singh, A.K.; McIntyre, L.M.; Sherman, L.A. Differential gene expression in response to hydrogen peroxide and the putative PerR regulon of *Synechocystis* sp. strain PCC 6803. *J. Bacteriol.* **2004**, *186*, 3331–3345. [CrossRef]
10. Kanesaki, Y.; Yamamoto, H.; Paithoonrangsarid, K.; Shoumskaya, M.; Suzuki, I.; Hayashi, H.; Murata, N. Histidine kinases play important roles in the perception and signal transduction of hydrogen peroxide in the cyanobacterium, *Synechocystis* sp. PCC 6803. *Plant J. Cell Mol. Biol.* **2007**, *49*, 313–324. [CrossRef]
11. Kobayashi, M.; Ishizuka, T.; Katayama, M.; Kanehisa, M.; Bhattacharyya-Pakrasi, M.; Pakrasi, H.B.; Ikeuchi, M. Response to Oxidative stress involves a novel peroxiredoxin gene in the unicellular cyanobacterium *Synechocystis* sp. PCC 6803. *Plant Cell Physiol.* **2004**, *45*, 290–299. [CrossRef]
12. Latifi, A.; Ruiz, M.; Zhang, C.C. Oxidative stress in cyanobacteria. *FEMS Microbiol. Rev.* **2009**, *33*, 258–278. [CrossRef]
13. Xia, Y.; Lü, C.; Hou, N.; Xin, Y.; Liu, J.; Liu, H.; Xun, L. Sulfide production and oxidation by heterotrophic bacteria under aerobic conditions. *ISME J.* **2017**, *11*, 2754–2766. [CrossRef]
14. Li, K.; Xin, Y.; Xuan, G.; Zhao, R.; Liu, H.; Xia, Y.; Xun, L. *Escherichia coli* uses separate enzymes to produce H_2S and Reactive Sulfane Sulfur from L-cysteine. *Front. Microbiol.* **2019**, *10*, 298. [CrossRef]
15. Xin, Y.; Liu, H.; Cui, F.; Liu, H.; Xun, L. Recombinant *Escherichia coli* with sulfide:quinone oxidoreductase and persulfide dioxygenase rapidly oxidises sulfide to sulfite and thiosulfate via a new pathway. *Environ. Microbiol.* **2016**, *18*, 5123–5136. [CrossRef]
16. Wang, R. Physiological implications of hydrogen sulfide: A whiff exploration that blossomed. *Physiol. Rev.* **2012**, *92*, 791–896. [CrossRef]
17. Xuan, G.; Lü, C.; Xu, H.; Chen, Z.; Li, K.; Liu, H.; Liu, H.; Xia, Y.; Xun, L. Sulfane Sulfur is an intrinsic signal activating MexR-regulated antibiotic resistance in *Pseudomonas aeruginosa*. *Mol. Microbiol.* **2020**, *114*, 1038–1048. [CrossRef]

18. Xuan, G.; Lv, C.; Xu, H.; Li, K.; Liu, H.; Xia, Y.; Xun, L. Sulfane sulfur regulates LasR-mediated quorum sensing and virulence in *Pseudomonas aeruginosa* PAO1. *Antioxidants* **2021**, *10*, 1498. [CrossRef]

19. Xun, H.; Xuan, G.; Liu, H.; Xia, Y.; Xun, L. Sulfane sulfur is a strong inducer of the multiple antibiotic resistance regulator MarR in *Escherichia coli*. *Antioxidants* **2021**, *10*, 1778. [CrossRef]

20. Iciek, M.; Kowalczyk-Pachel, D.; Bilska-Wilkosz, A.; Kwiecien, I.; Gorny, M.; Wlodek, L. S-sulfhydration as a cellular redox regulation. *Biosci. Rep.* **2015**, *36*, e00304. [CrossRef]

21. Yan, F.; Fojtikova, V.; Man, P.; Stranava, M.; Martínková, M.; Du, Y.; Huang, D.; Shimizu, T. Catalytic enhancement of the heme-based oxygen-sensing phosphodiesterase EcDOS by hydrogen sulfide is caused by changes in heme coordination structure. *Biomet. Int. J. Role Met. Ions Biol. Biochem. Med.* **2015**, *28*, 637–652. [CrossRef]

22. Zivanovic, J.; Kouroussis, E.; Kohl, J.B.; Adhikari, B.; Bursac, B.; Schott-Roux, S.; Petrovic, D.; Miljkovic, J.L.; Thomas-Lopez, D.; Jung, Y.; et al. Selective persulfide detection reveals evolutionarily conserved antiaging effects of s-sulfhydration. *Cell Metab.* **2019**, *30*, 1152–1170.e13. [CrossRef]

23. Bhatwalkar, S.B.; Mondal, R.; Krishna, S.B.N.; Adam, J.K.; Govender, P.; Anupam, R. Antibacterial properties of organosulfur compounds of Garlic (*Allium sativum*). *Front. Microbiol.* **2021**, *12*, 613077. [CrossRef]

24. Liu, D.; Zhang, J.; Lü, C.; Xia, Y.; Liu, H.; Jiao, N.; Xun, L.; Liu, J. *Synechococcus* sp. strain PCC7002 uses Sulfide:Quinone Oxidoreductase to detoxify exogenous sulfide and to convert endogenous sulfide to cellular sulfane sulfur. *mBio* **2020**, *11*, e03420–e03519. [CrossRef]

25. Liu, H.; Xin, Y.; Xun, L. Distribution, diversity, and activities of sulfur dioxygenases in heterotrophic bacteria. *Appl. Environ. Microbiol.* **2014**, *80*, 1799–1806. [CrossRef]

26. Lü, C.; Xia, Y.; Liu, D.; Zhao, R.; Gao, R.; Liu, H.; Xun, L. *Cupriavidus necator* H16 uses flavocytochrome c sulfide dehydrogenase to oxidize self-produced and added sulfide. *Appl. Environ. Microbiol.* **2017**, *83*, e01610–e01617. [CrossRef]

27. Harada, M.; Akiyama, A.; Furukawa, R.; Yokobori, S.I.; Tajika, E.; Yamagishi, A. Evolution of superoxide dismutases and catalases in cyanobacteria: Occurrence of the antioxidant enzyme genes before the rise of atmospheric oxygen. *J. Mol. Evol.* **2021**, *89*, 527–543. [CrossRef]

28. Olson, K.R.; Gao, Y.; DeLeon, E.R.; Arif, M.; Arif, F.; Arora, N.; Straub, K.D. Catalase as a sulfide-sulfur oxido-reductase: An ancient (and modern?) regulator of reactive sulfur species (RSS). *Redox Biol.* **2017**, *12*, 325–339. [CrossRef]

29. Olson, K.R.; Gao, Y.; Arif, F.; Arora, K.; Patel, S.; DeLeon, E.R.; Sutton, T.R.; Feelisch, M.; Cortese-Krott, M.M.; Straub, K.D. Metabolism of hydrogen sulfide (H_2S) and Production of Reactive Sulfur Species (RSS) by superoxide dismutase. *Redox Biol.* **2018**, *15*, 74–85. [CrossRef]

30. Hou, N.; Yan, Z.; Fan, K.; Li, H.; Zhao, R.; Xia, Y.; Xun, L.; Liu, H. OxyR senses sulfane sulfur and activates the genes for its removal in Escherichia coli. *Redox Biol.* **2019**, *26*, 101293. [CrossRef]

31. Liu, D.; Chen, J.; Wang, Y.; Meng, Y.; Li, Y.; Huang, R.; Xia, Y.; Liu, H.; Jiao, N.; Xun, L.; et al. *Synechococcus* sp. PCC7002 uses peroxiredoxin to cope with reactive sulfur species stress. *mBio* **2022**, *13*, e0103922. [CrossRef] [PubMed]

32. Marinho, H.S.; Real, C.; Cyrne, L.; Soares, H.; Antunes, F. Hydrogen peroxide sensing, signaling and regulation of transcription factors. *Redox Biol.* **2014**, *2*, 535–562. [CrossRef]

33. Luebke, J.L.; Shen, J.; Bruce, K.E.; Kehl-Fie, T.E.; Peng, H.; Skaar, E.P.; Giedroc, D.P. The CsoR-like sulfurtransferase repressor (CstR) is a persulfide sensor in *Staphylococcus aureus*. *Mol. Microbiol.* **2014**, *94*, 1343–1360. [CrossRef] [PubMed]

34. Guimarães, B.G.; Barbosa, R.L.; Soprano, A.S.; Campos, B.M.; de Souza, T.A.; Tonoli, C.C.C.; Leme, A.F.P.; Murakami, M.T.; Benedetti, C.E. Plant pathogenic bacteria utilize biofilm growth-associated repressor (BigR), a novel winged-helix redox switch, to control hydrogen sulfide detoxification under hypoxia. *J. Biol. Chem.* **2011**, *286*, 26148–26157. [CrossRef]

35. Shimizu, T.; Shen, J.; Fang, M.; Zhang, Y.; Hori, K.; Trinidad, J.C.; Bauer, C.E.; Giedroc, D.P.; Masuda, S. Sulfide-responsive transcriptional repressor SqrR functions as a master regulator of sulfide-dependent photosynthesis. *Proc. Natl. Acad. Sci. USA* **2017**, *114*, 2355–2360. [CrossRef]

36. Li, H.; Li, J.; Lu, C.; Xia, Y.; Xin, Y.; Liu, H.; Xun, L.; Liu, H. FisR activates sigma(54)-dependent transcription of sulfide-oxidizing genes in *Cupriavidus pinatubonensis* JMP134. *Mol. Microbiol.* **2017**, *105*, 373–384. [CrossRef]

37. Jo, I.; Chung, I.Y.; Bae, H.W.; Kim, J.S.; Song, S.; Cho, Y.H.; Ha, N.C. Structural details of the OxyR peroxide-sensing mechanism. *Proc. Natl. Acad. Sci. USA* **2015**, *112*, 6443–6448. [CrossRef]

38. Lee, J.W.; Helmann, J.D. The PerR transcription factor senses H_2O_2 by metal-catalysed histidine oxidation. *Nature* **2006**, *440*, 363–367. [CrossRef]

39. Lee, J.W.; Helmann, J.D. Biochemical characterization of the structural Zn^{2+} site in the *Bacillus subtilis* peroxide sensor PerR. *J. Biol. Chem.* **2006**, *281*, 23567–23578. [CrossRef]

40. Ludwig, M.; Chua, T.T.; Chew, C.Y.; Bryant, D.A. Fur-type transcriptional repressors and metal homeostasis in the cyanobacterium *Synechococcus* sp. PCC 7002. *Front. Microbiol.* **2015**, *6*, 1217. [CrossRef]

41. Ida, T.; Sawa, T.; Ihara, H.; Tsuchiya, Y.; Watanabe, Y.; Kumagai, Y.; Suematsu, M.; Motohashi, H.; Fujii, S.; Matsunaga, T.; et al. Reactive cysteine persulfides and S-polythiolation regulate oxidative stress and redox signaling. *Proc. Natl. Acad. Sci. USA* **2014**, *111*, 7606–7611. [CrossRef]

42. Stevens, S.E.; Porter, R.D. Transformation in Agmenellum quadruplicatum. *Proc. Natl. Acad. Sci. USA* **1980**, *77*, 6052–6056. [CrossRef]

43. Xia, Y.; Li, K.; Li, J.; Wang, T.; Gu, L.; Xun, L. T5 exonuclease-dependent assembly offers a low-cost method for efficient cloning and site-directed mutagenesis. *Nucleic Acids Res.* **2019**, *47*, e15. [CrossRef]

44. Nagy, P.; Pálinkás, Z.; Nagy, A.; Budai, B.; Tóth, I.; Vasas, A. Chemical aspects of hydrogen sulfide measurements in physiological samples. *Biochim. Biophys. Acta* **2014**, *1840*, 876–891. [CrossRef]

45. Szekeres, E.; Sicora, C.; Dragos, N.; Druga, B. Selection of proper reference genes for the cyanobacterium *Synechococcus* PCC 7002 using real-time quantitative PCR. *FEMS Microbiol. Lett.* **2014**, *359*, 102–109. [CrossRef]

46. Livak, K.J.; Schmittgen, T.D. Analysis of relative gene expression data using real-time quantitative PCR and the 2(-Delta Delta C(T)) Method. *Methods* **2001**, *25*, 402–408. [CrossRef]

47. Xia, Y.; Xun, L. Revised mechanism and improved efficiency of the quikchange site-directed mutagenesis method. *Methods Mol. Biol.* **2017**, *1498*, 367–374. [CrossRef]

48. Waugh, D.S. The remarkable solubility-enhancing power of *Escherichia coli* maltose-binding protein. *Postep. Biochem.* **2016**, *62*, 377–382. [CrossRef]

49. Lu, T.; Cao, Q.; Pang, X.; Xia, Y.; Xun, L.; Liu, H. Sulfane sulfur-activated actinorhodin production and sporulation is maintained by a natural gene circuit in *Streptomyces coelicolor*. *Microb. Biotechnol.* **2020**, *13*, 1917–1932. [CrossRef]

50. Doka, E.; Pader, I.; Biro, A.; Johansson, K.; Cheng, Q.; Ballago, K.; Prigge, J.R.; Pastor-Flores, D.; Dick, T.P.; Schmidt, E.E.; et al. A novel persulfide detection method reveals protein persulfide- and polysulfide-reducing functions of thioredoxin and glutathione systems. *Sci. Adv.* **2016**, *2*, e1500968. [CrossRef]

51. Fan, K.; Chen, Z.; Liu, H. Evidence that the ProPerDP method is inadequate for protein persulfidation detection due to lack of specificity. *Sci. Adv.* **2020**, *6*, eabb6477. [CrossRef]

52. Dóka, É.; Arnér, E.S.J.; Schmidt, E.E.; Dick, T.P.; van der Vliet, A.; Yang, J.; Szatmári, R.; Ditrói, T.; Wallace, J.L.; Cirino, G.; et al. Comment on "Evidence that the ProPerDP method is inadequate for protein persulfidation detection due to lack of specificity". *Sci. Adv.* **2021**, *7*, abe7006. [CrossRef] [PubMed]

53. Gerdol, M.; Sollitto, M.; Pallavicini, A.; Castellano, I. The complex evolutionary history of sulfoxide synthase in ovothiol biosynthesis. *Proc. Biol. Sci.* **2019**, *286*, 20191812. [CrossRef] [PubMed]

54. Katoh, K.; Standley, D.M. MAFFT multiple sequence alignment software version 7: Improvements in performance and usability. *Mol. Biol. Evol.* **2013**, *30*, 772–780. [CrossRef] [PubMed]

55. Capella-Gutiérrez, S.; Silla-Martínez, J.M.; Gabaldón, T. trimAl: A tool for automated alignment trimming in large-scale phylogenetic analyses. *Bioinformatics* **2009**, *25*, 1972–1973. [CrossRef] [PubMed]

56. Naser-Khdour, S.; Minh, B.Q.; Lanfear, R. Assessing confidence in root placement on phylogenies: An empirical study using non-reversible models for mammals. *Syst. Biol.* **2021**, *71*, 959–972. [CrossRef]

57. Kalyaanamoorthy, S.; Minh, B.Q.; Wong, T.K.F.; von Haeseler, A.; Jermiin, L.S. ModelFinder: Fast model selection for accurate phylogenetic estimates. *Nat. Methods* **2017**, *14*, 587–589. [CrossRef] [PubMed]

58. MacPherson, S.; Larochelle, M.; Turcotte, B. A fungal family of transcriptional regulators: The zinc cluster proteins. *Microbiol. Mol. Biol. Rev.* **2006**, *70*, 583–604. [CrossRef]

59. Laity, J.H.; Lee, B.M.; Wright, P.E. Zinc finger proteins: New insights into structural and functional diversity. *Curr. Opin. Struct. Biol.* **2001**, *11*, 39–46. [CrossRef]

60. Näär, A.M.; Ryu, S.; Tjian, R. Cofactor requirements for transcriptional activation by Sp1. *Cold Spring Harb. Symp. Quant. Biol.* **1998**, *63*, 189–199. [CrossRef]

61. Urnov, F.D. A feel for the template: Zinc finger protein transcription factors and chromatin. *Biochem. Cell Biol.* **2002**, *80*, 321–333. [CrossRef] [PubMed]

62. Todd, R.B.; Andrianopoulos, A. Evolution of a fungal regulatory gene family: The Zn(II)2Cys6 binuclear cluster DNA binding motif. *Fungal Genet. Biol.* **1997**, *21*, 388–405. [CrossRef] [PubMed]

63. Kim, S.O.; Merchant, K.; Nudelman, R.; Beyer, W.F.; Keng, T.; DeAngelo, J.; Hausladen, A.; Stamler, J.S. OxyR: A molecular code for redox-related signaling. *Cell* **2002**, *109*, 383–396. [CrossRef] [PubMed]

64. Choi, H.-J.; Kim, S.-J.; Mukhopadhyay, P.; Cho, S.; Woo, J.-R.; Storz, G.; Ryu, S.-E. Structural basis of the redox switch in the OxyR transcription factor. *Cell* **2001**, *105*, 103–113. [CrossRef]

65. Storz, G.; Tartaglia, L.A.; Ames, B.N. Transcriptional regulator of oxidative stress-inducible genes: Direct activation by oxidation. *Science* **1990**, *248*, 189–194. [CrossRef]

66. Tseng, H.J.; McEwan, A.G.; Apicella, M.A.; Jennings, M.P. OxyR acts as a repressor of catalase expression in *Neisseria gonorrhoeae*. *Infect. Immun.* **2003**, *71*, 550–556. [CrossRef]

67. Wu, H.J.; Seib, K.L.; Srikhanta, Y.N.; Kidd, S.P.; Edwards, J.L.; Maguire, T.L.; Grimmond, S.M.; Apicella, M.A.; McEwan, A.G.; Jennings, M.P. PerR controls Mn-dependent resistance to oxidative stress in *Neisseria gonorrhoeae*. *Mol. Microbiol.* **2006**, *60*, 401–416. [CrossRef]

68. Ashby, M.K.; Houmard, J. Cyanobacterial two-component proteins: Structure, diversity, distribution, and evolution. *Microbiol. Mol. Biol. Rev.* **2006**, *70*, 472–509. [CrossRef]

69. Koskinen, S.; Hakkila, K.; Kurkela, J.; Tyystjärvi, E.; Tyystjärvi, T. Inactivation of group 2 σ factors upregulates production of transcription and translation machineries in the cyanobacterium *Synechocystis* sp. PCC 6803. *Sci. Rep.* **2018**, *8*, 10305. [CrossRef]

70. Grettenberger, C.L. Novel *Gloeobacterales* spp. from diverse environments across the globe. *mSphere* **2021**, *6*, e0006121. [CrossRef]

71. Briand, J.-F.; Robillot, C.; Quiblier, C.; Bernard, C. A perennial bloom of planktothrix agardhii (cyanobacteria) in a shallow eutrophic french lake: Limnological and microcystin production studies. *Arch. Fur Hydrobiol.* **2002**, *153*, 605–622. [CrossRef]

72. Schunck, H.; Lavik, G.; Desai, D.K.; Grosskopf, T.; Kalvelage, T.; Loscher, C.R.; Paulmier, A.; Contreras, S.; Siegel, H.; Holtappels, M.; et al. Giant hydrogen sulfide plume in the oxygen minimum zone off Peru supports chemolithoautotrophy. *PLoS ONE* **2013**, *8*, e68661. [CrossRef]

73. Klatt, J.M.; Gomez-Saez, G.V.; Meyer, S.; Ristova, P.P.; Yilmaz, P.; Granitsiotis, M.S.; Macalady, J.L.; Lavik, G.; Polerecky, L.; Bühring, S.I. Versatile cyanobacteria control the timing and extent of sulfide production in a Proterozoic analog microbial mat. *ISME J.* **2020**, *14*, 3024–3037. [CrossRef] [PubMed]

74. Stal, L.J.; Moezelaar, R. Fermentation in cyanobacteria. *FEMS Microbiol. Rev.* **1997**, *21*, 179–211. [CrossRef]

75. Klatt, J.M.; de Beer, D.; Hausler, S.; Polerecky, L. Cyanobacteria in sulfidic spring microbial mats can perform oxygenic and anoxygenic photosynthesis simultaneously during an entire diurnal period. *Front. Microbiol.* **2016**, *7*, 1973. [CrossRef]

76. Liao, C.; Seebeck, F.P. Convergent evolution of ergothioneine biosynthesis in cyanobacteria. *ChemBioChem* **2017**, *18*, 2115–2118. [CrossRef]

77. Brancaccio, M.; Tangherlini, M.; Danovaro, R.; Castellano, I. Metabolic adaptations to marine environments: Molecular diversity and evolution of ovothiol biosynthesis in bacteria. *Genome Biol. Evol.* **2021**, *13*, evab169. [CrossRef]

78. Sevilla, E.; Sarasa-Buisan, C.; Gonzalez, A.; Cases, R.; Kufryk, G.; Peleato, M.L.; Fillat, M.F. Regulation by FurC in *Anabaena* links the oxidative stress response to photosynthetic metabolism. *Plant Cell Physiol.* **2019**, *60*, 1778–1789. [CrossRef]